JCTC Journal of Chemical Theory and Computation

Article

pubs.acs.org/JCTC

Generalized Born and Explicit Solvent Models for Free Energy Calculations in Organic Solvents: Cyclodextrin Dimerization

Haiyang Zhang,[†,‡] Tianwei Tan,[‡] and David van der Spoel[*,§]

[†]Department of Biological Science and Engineering, School of Chemistry and Biological Engineering, University of Science and Technology Beijing, 100083 Beijing, China

[‡]Beijing Key Laboratory of Bioprocess, Department of Biochemical Engineering, Beijing University of Chemical Technology, Box 53, 100029 Beijing, China

[§]Uppsala Center for Computational Chemistry, Science for Life Laboratory, Department of Cell and Molecular Biology, Uppsala University, Husargatan 3, Box 596, SE-75124 Uppsala, Sweden

Supporting Information

ABSTRACT: Evaluation of solvation (binding) free energies with implicit solvent models in different dielectric environments for biological simulations as well as high throughput ligand screening remain challenging endeavors. In order to address how well implicit solvent models approximate explicit ones we examined four generalized Born models (GB^{Still}, GB^{HCT}, $GB^{OBC}I$, and $GB^{OBC}II$) for determining the dimerization free energy (ΔG^0) of β-cyclodextrin monomers in 17 implicit solvents with dielectric constants (D) ranging from 5 to 80 and compared the results to previous free energy calculations with explicit solvents (Zhang et al. *J. Phys. Chem. B* **2012**, *116*, 12684−12693). The comparison indicates that neglecting the environmental dependence of Born radii appears acceptable for such calculations involving cyclodextrin and that the GB^{Still} and $GB^{OBC}I$ models yield a reasonable estimation of ΔG^0, although the details of binding are quite different from explicit solvents. Large discrepancies between implicit and explicit solvent models occur in high-dielectric media with strong hydrogen bond (HB) interruption properties. ΔG^0 with the GB models is shown to correlate strongly to $2(D-1)/(2D+1)$ ($R^2 \sim 0.90$) in line with the Onsager reaction field (Onsager *J. Am. Chem. Soc.* **1936**, *58*, 1486−1493) but to be very sensitive to D ($D < 10$) as well. Both high-dielectric environments where hydrogen bonds are of interest and low-dielectric media such as protein binding pockets and membrane interiors therefore need to be considered with caution in GB-based calculations. Finally, a literature analysis of Gibbs energy of solvation of small molecules in organic liquids shows that the Onsager relation does not hold for real molecules since the correlation between ΔG^0 and $2(D-1)/(2D+1)$ is low for most solutes. Interestingly, explicit solvent calculations of the solvation free energy (Zhang et al. *J. Chem. Inf. Model.* **2015**, *55*, 1192−1201) reproduce the weak experimental correlations with $2(D-1)/(2D+1)$ very well.

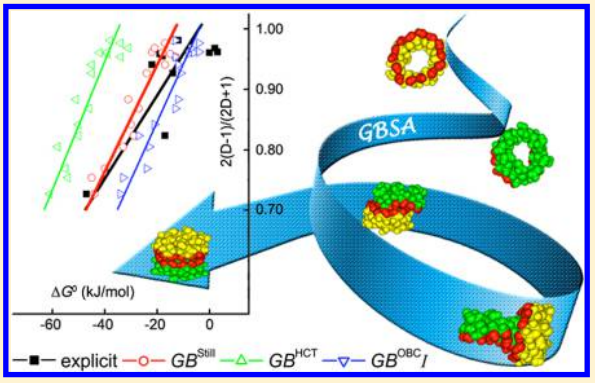

INTRODUCTION

The free energy of binding (ΔG_{bind}) of for instance a protein and a ligand is a crucial property within medicinal chemistry. Quantitative measurements of ΔG_{bind} are tedious and often expensive to perform, and therefore computational investigations can be an alternative. A range of different computational methods are available that can be categorized into methods using explicit solvent molecules and methods using an implicit description of the solvent. The latter category has been developed predominantly in order to reduce computational costs.[1−3] In most implicit solvent models the solvent is treated as a continuous medium with certain dielectric and interfacial properties. Compared with explicit solvent calculations, such treatment reduces the number of interacting particles and degrees of freedom in a system and provides a reasonably efficient representation of the long-range electrostatic effects from solvent molecules. Though further improvements are desirable in some cases and work on this is indeed ongoing,[4] implicit solvation models have been used for many applications such as simulations of protein dynamics[5−7] and prediction of ligand binding.[8−10] An obvious limitation of implicit solvents is that short-range interactions and solvent orientation (e.g., hydrogen bonds) are poorly modeled (except for the case of symmetric solvent molecules like CCl_4). This means that solvent effects due to details of liquid structure at interfaces (including air−liquid and protein-liquid interfaces) are washed out.

In popular implicit solvent models, the solvation free energy (ΔG_{sol}) is typically given as the sum of a solute−solvent electrostatic polarization term (ΔG_{pol}) having a significant (in high dielectric solvents) contribution to ΔG_{sol} and of a

Received: June 30, 2015
Published: September 30, 2015

DOI: 10.1021/acs.jctc.5b00620
J. Chem. Theory Comput. 2015, 11, 5103−5113

nonpolar one (ΔG_{np}). ΔG_{np} can be further decomposed into two components: a solvent−solvent cavity term for solute accommodation (ΔG_{cav}) and a solute−solvent van der Waals contribution (ΔG_{vdw}) (eq 1).[4]

$$\Delta G_{sol} = \Delta G_{pol} + \Delta G_{np} = \Delta G_{pol} + (\Delta G_{cav} + \Delta G_{vdw}) \quad (1)$$

The electrostatic term can be evaluated quite accurately using dielectric continuum methods based on the numerical solution to the Poisson−Boltzmann (PB) equation.[11,12] Due to the high computational cost of PB electrostatics algorithms, in practice often simpler approximations are used, in particular, generalized Born (GB) models that estimate the dielectric descreening in terms of the known Born radii for quantifying the degree of burial of individual atoms.[13−15] ΔG_{np} is generally evaluated from the total solvent-accessible surface area (SA) scaled by a surface tension. Together with ΔG_{pol}, these make up the well-known PB/SA and GB/SA schemes. Comparative studies on the GB method have indicated that it is possible to reproduce the reference PB model with good accuracy.[16−18] A recent report on protein folding simulations using GB models showed that implicit solvent models are sufficiently accurate to find the native structure of proteins,[7] although earlier studies found that explicit solvent locates native structures more reliably.[19−21]

GB solvent approximations have been extensively used in high-throughput screening to score protein−ligand complexes, in combination with molecular mechanics (MM) force fields.[22−24] An integration of GB models in molecular dynamics (MD) packages further allows investigating large-scale biological phenomena, in particular, for instance conformational transitions in proteins and protein complexes.[25] Consequently, a multitude of GB-based investigations into protein dynamics and ligand binding have been published, as well as the comparison with explicit solvent results and experimental observations. For instance, Honig and co-workers reported a comparative MD study of three GB models on protein structures, highlighting the necessity for evaluating the effects of different models on the simulation results.[26] Using an improved GB solvent model, Simmerling et al. recently presented *ab initio* folding of 17 proteins with 10−92 amino acids and concluded that all tested proteins but one could be folded accurately in days.[7] They also suggested that the low thermal stability existing in their model could be improved by tuning of the ΔG_{np} contribution. Zeller and Zacharias evaluated the accuracy of GB models for free energy calculations on binding of small peptide ligands to a protein receptor and concluded that recent GB models can compete with explicit solvent results in ΔG_{bind} if no charged residues are present at the binding interface.[27]

Despite the lower demands on computer time and successful applications, the reports mentioned above indicate that for current GB solvent parameters further improvements and more systematic benchmarks are required. Another point of concern is that almost all GB-based calculations reported focus on the molecular properties, such as binding or solvation free energies, in aqueous solution. Indeed there are few force field benchmarks on free energy of solvation in other (explicit) solvents than water as well.[28,29] For many biological and pharmaceutical applications, however, there are other media, like nucleic acids and phospholipid bilayers, having very different dielectric properties from water that are equally important and have not been addressed sufficiently.[2,4,30,31]

The question we address in this work is how well GB models approximate different explicit solvents, with varying dielectric properties. Following our previous work on the dimerization of β-cyclodextrin (β-CD) monomers in ten explicit solvents,[32] here we present an extensive determination of the dimerization free energy of β-CD monomers in 17 implicit solvents and compare them to the previous explicit solvent calculations. β-CD dimer was chosen as a model because β-CD is an ideal host (receptor) candidate for use in pharmaceutical applications like drug delivery[33] as well as for mimicking protein−ligand interactions.[34] The hydrogen bonding (HB) interactions responsible for cyclodextrin dimerization are ubiquitous in biomolecular structures as well and are crucial for instance for protein aggregations.[35] The GB methods examined here include Still,[36] Hawkins-Cramer-Truhlar (HCT),[37] and Onufriev-Bashford-Case (OBC)[38] models, here referred to as GB^{Still}, GB^{HCT}, and GB^{OBC}, respectively. Potentials of mean force (i.e., free energy profiles) for the β-CD dimerization process were computed using umbrella sampling simulations, from which we obtained the dimerization free energy (ΔG^0) of two β-CD monomers. The relationship between ΔG^0 and dielectric constants for different GB models was evaluated and compared to explicit solvent results. Binding energies along the dimerization coordinate were further decomposed for a better understanding of the energy landscape and for a detailed comparison of implicit solvent results with explicit ones. General implications for GB-based calculations are discussed in the end. This work provides valuable insights into the use of implicit solvent models in not just water but other environments and may lead to suggestions for improvement of GB models in different dielectric environments.

METHODS

Dielectric Constant Setup. A total of 17 organic solvents with dielectric constants ranging from 5 to 80 are examined; these solvents include water (HOH), methanol (MeOH), ethanol (EtOH), dimethyl sulfoxide (DMSO), *N,N*-dimethylacetamide (DMA), *N,N*-dimethylformamide (DMF), acetone (ACO), tetrahydrofuran (THF), acetonitrile (ACN), chloroform ($CHCl_3$), chlorobenzene (CB), ethyl acetate (EA), 1,2-dimethoxyethane (DME), dichloromethane (DCM), *tert*-butyl alcohol (TBA), pyridine (PRD), and propylene carbonate (PC). Explicit solvent simulations for the first 10 solvents have been presented in our previous study[32] and are used in this work for a direct comparison with implicit calculations. The last seven solvents were added to ensure a diversity of dielectric constants; the diversity refers to Figure S1 in the Supporting Information. All the dielectric constants tested and their reference solvents are given in Table 1.

Simulation Protocol. The initial coordinate of β-CD head-to-head dimer was extracted from the Cambridge Crystallo-

Table 1. Dielectric Constant (D) for GB Solvent Models

solvent	D	solvent	D	solvent	D
$CHCl_3$[a]	5	TBA	10.9	DMF[a]	38
CB	5.6	PRD	12.4	DMA[a]	39
EA	6	ACO[a]	20	DMSO[a]	47
DME	7.2	EtOH[a]	25	PC	64
THF[a]	8	MeOH[a]	33	HOH[a]	80
DCM	9	ACN[a]	36		

[a]Explicit calculations available for comparison.[32]

DOI: 10.1021/acs.jctc.5b00620
J. Chem. Theory Comput. 2015, 11, 5103−5113

graphic Data Centre (CCDC no. 785103).[39] Implicit solvent simulations with the GB formalism were performed at 300 *K* using the GROMACS package (version 4.5.5).[40−42] The simulations were implemented without periodic boundary conditions and without cut-offs (all-vs-all) for both electrostatic and van der Waals interactions. The velocity rescaling thermostat[43] was applied with a coupling constant of 0.1 ps for temperature coupling, and no pressure coupling was imposed due to the vacuum boundary conditions. The bond lengths of β-CD were constrained with the LINCS algorithm.[44] β-CD was modeled by the q4md-CD force field,[32,45] and three different solvent models available in the GROMACS suite,[46] namely, GB^{Still},[36] GB^{HCT},[37] and GB^{OBC},[38] were adopted to represent the continuous media. The set of van der Waals radii used in the calculation of effective Born radii is given in the Supporting Information. The polar solvation part (ΔG_{pol}) in eq 1 was derived from the generalized Born equation,[36,46] and the nonpolar part (ΔG_{np}) was computed directly from the Born radius of each atom with a simple ACE type approximation.[47]

Umbrella Sampling. After energy minimization, a center of mass (COM) pulling simulation was performed to obtain a dissociation process of β-CD dimer. The COM distance between two β-CD monomers along the *Z*-axis was defined to be the reaction coordinate ξ (Figure 1).

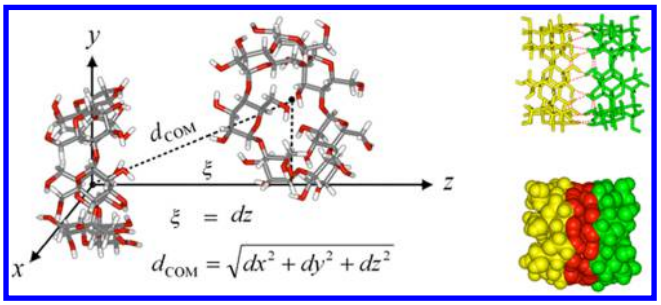

Figure 1. Definition of the reaction coordinate ξ for β-CD dimerization (left) and β-CD dimers shown with stick (upper right) and space-filling (lower right) models. For the monomers (left), gray sticks are carbon atoms, red for oxygen, and white for hydrogen. Dotted red lines and red balls (right) indicate hydrogen bond networks.

Along ξ, we then selected ~40 windows in the [0.60, 1.60] interval with a distance equal to 0.025 nm between adjacent positions, and these windows were adopted for subsequent umbrella sampling simulations. Full details on the COM pulling and umbrella sampling simulations have been presented in ref 32. Each window was simulated for 20 ns, and this was enough for convergence of the resulting potential of mean force (PMF) profile (Figure S2 in the Supporting Information). The overall simulation time for a single PMF is about 800 ns. Following the same procedure, β-CD dimerization was simulated in 17 organic solvents with *D* listed in Table 1 for GB^{Still}, GB^{HCT}, and GB^{OBC}, respectively. Since GB^{OBC} has two parameter sets (refer to $GB^{OBC}I$ and $GB^{OBC}II$),[38] a total of 68 PMF profiles was therefore obtained with a total simulation time of 54.4 μs.

Energetic Analysis. The first 2 ns simulations were discarded for equilibration, and the remaining 18 ns were used for data collection. PMFs, $\Delta G(\xi)$, for β-CD dimerization were constructed with the weighted histogram analysis method (WHAM).[48,49] Statistical errors of the PMFs were estimated by the Bayesian bootstrapping of complete histograms.[49] All the PMFs were defined to zero at ξ = 1.55 nm where two β-CD monomers were completely separated.

The binding constant (K_a) of two β-CD monomers can be computed using eq 2

$$K_a = \pi N_A \int r(\xi)^2 \exp[-\Delta G(\xi)/RT] d\xi \quad (2)$$

where N_A is Avogadro constant, *R* is the ideal gas constant, and $\pi r(\xi)^2$ is the sampled area for the centroid of β-CD monomer in the *X*-*Y* plane at ξ.[50,51] The standard binding free energy of β-CD dimerization (ΔG^0) can therefore be derived from eq 3

$$\Delta G^\circ = -RT \ln(K_a C^0) \quad (3)$$

where C^0 is the standard concentration of 1 mol/L.

For a detailed understanding of the dimerization process with the GB models, we define a binding energy of two β-CD monomers along ξ, $\Delta E(\xi)$, to be the potential energy difference with respect to the separated state of the binding partners. ΔE can be further decomposed into five terms (eq 4)

$$\Delta E = \Delta E_b + \Delta E_{nb\text{-}intra} + \Delta E_{nb\text{-}inter} + \Delta E_{pol} + \Delta E_{np} \quad (4)$$

ΔE_b denotes bonded interactions, $\Delta E_{nb\text{-}intra}$ denotes nonbonded intramolecular interactions, and $\Delta E_{nb\text{-}inter}$ denotes nonbonded intermolecular interactions (between β-CD monomers). ΔE_{pol} and ΔE_{np} represent polar and nonpolar parts of solvation contributions, respectively. For comparison, ΔE for explicit solvent simulations was also decomposed in a similar manner. Differences in the calculation of solvation interactions for explicit and implicit solvent models are listed in Table 2. The electrostatic interaction (ΔE_{ele}) between β-CDs and explicit solvents were used to compare the contribution of ΔE_{pol} in implicit calculations to. Note that each variable in eq 4 is a function of ξ, and this functional dependence is omitted here for simplicity. Error estimates of these variables were calculated using a binning analysis.[54]

Table 2. Calculation of Solvation Interactions in Explicit and Implicit Solvent Models

	solute−solvent		
solvent model	electrostatic	van der Waals	solvent−solvent
explicit[a]	ΔE_{ele}	ΔE_{vdw}	$\Delta E_{ele} + \Delta E_{vdw}$
implicit	ΔG_{pol} (GB equation)[36]	ΔG_{vdw}	ΔG_{cav}
		$\Delta G_{np} = \Delta G_{vdw} + \Delta G_{cav} = \sigma \cdot SA$[b]	

[a] ΔE_{ele} is computed by particle-mesh Eward (PME)[52,53] and ΔE_{vdw} by the Lennard-Jones function. [b] σ is a scaling factor for surface tension, and *SA* is the total solvent-accessible surface area.

RESULTS

PMF Profiles. Free energy files (PMFs) for β-CD dimerization with an implicit model of GB^{Still} are presented in Figure 2, and the results for explicit simulations are given for comparison. For $CHCl_3$ (D = 5) and HOH (D = 80), GB^{Still} yields PMF landscapes in reasonable agreement with explicit solvent models. However, there is significant discrepancy for the other solvents. As shown in Figure 2, GB^{Still} tends to overestimate the stability of the β-CD dimer in high polar solvents and to underestimate stability in the solvents with lower polarity. For instance, the gross overestimation of GB^{Still} yields a stable dimer in DMSO, DMA, and DMF (Figure 2),

DOI: 10.1021/acs.jctc.5b00620
J. Chem. Theory Comput. 2015, 11, 5103−5113

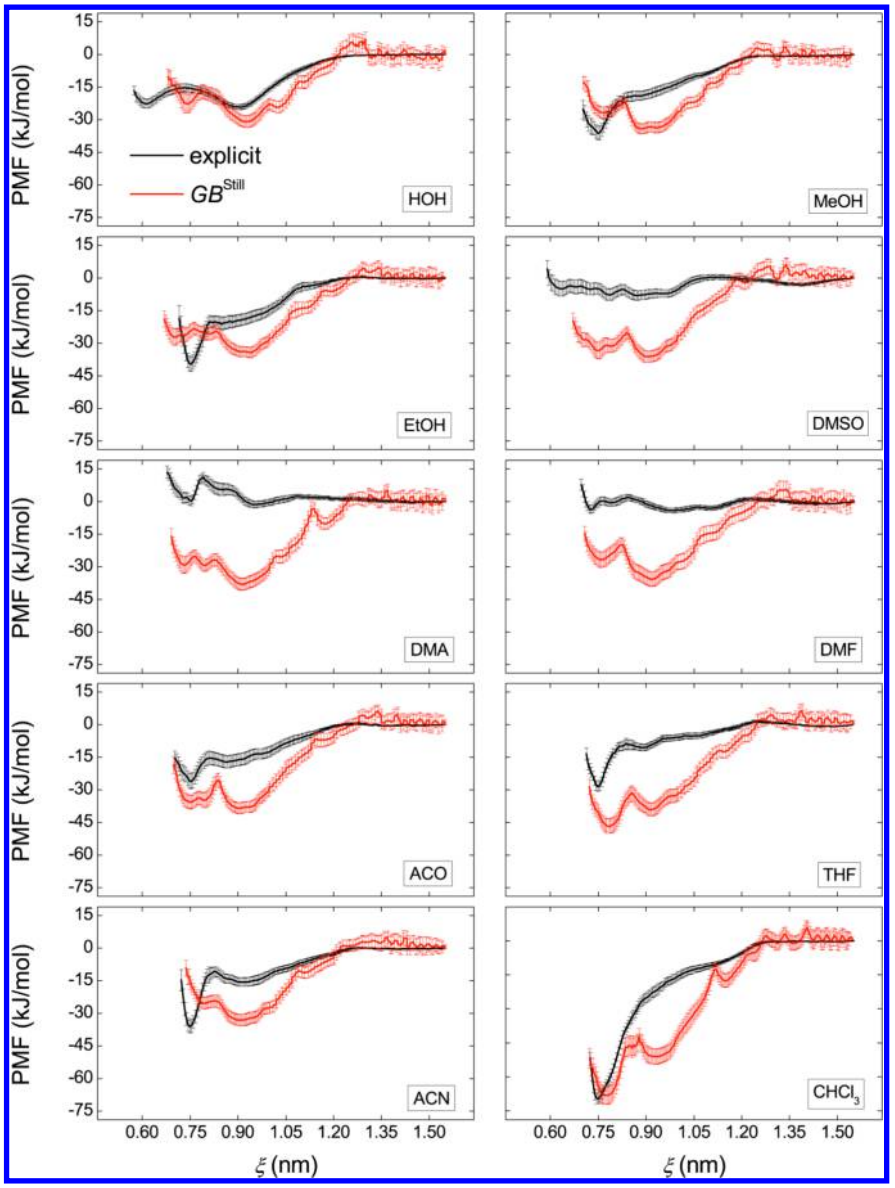

Figure 2. Comparison of PMF profiles in explicit solvents (black) with implicit GB^{Still} ones (red) for β-CD dimerization.

while explicit calculations show the opposite indicated by a non-negative $\Delta G(\xi)$. THF is an exceptional case; GB^{Still} results in an obvious overestimation of β-CD dimer stability for this weak polar solvent. These discrepancies seem not unexpected since implicit solvent is inherently noisy (e.g., a broken HB cannot be replaced by a real solvent). THF can act as a HB acceptor and interrupt HB networks of a β-CD dimer shown in Figure 1,[32] thus leading to a weaker binding. This destabilizing effect is apparently not described accurately in continuous solvation models.

PMF profiles with GB^{Still} for the other seven solvents without explicit calculations for comparison are shown in Figure 3. The well depth of PMFs seems more negative for smaller dielectric constants (D), indicating that binding affinity of the two monomers decreases with the increasing D. The stability of β-CD dimer is very sensitive to the solvents with smaller D ranging from 5 to 9, as seen from Figure 3. All the PMFs for the 17 solvent systems tested with GB^{Still}, GB^{HCT}, $GB^{OBC}I$, and $GB^{OBC}II$ models are given in Figures S3 and S4 in the Supporting Information. $GB^{OBC}I$ shows similar performances to

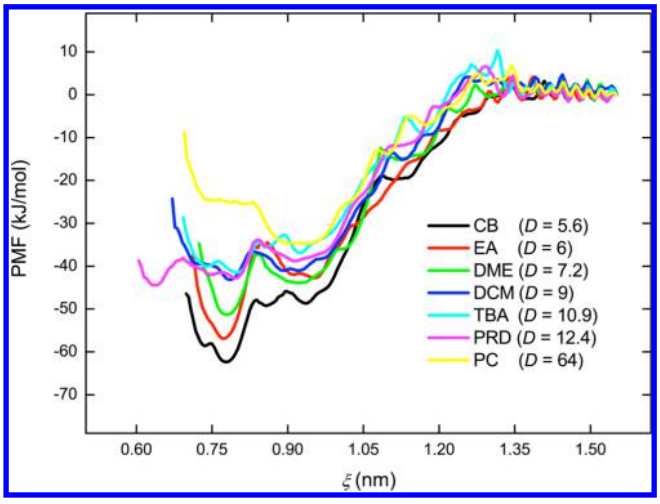

Figure 3. PMF profiles of β-CD dimerization with GB^{Still} for the tested solvents without explicit simulations available for comparison. Errors (~4 kJ/mol) are not shown here for clarity.

DOI: 10.1021/acs.jctc.5b00620
J. Chem. Theory Comput. 2015, 11, 5103−5113

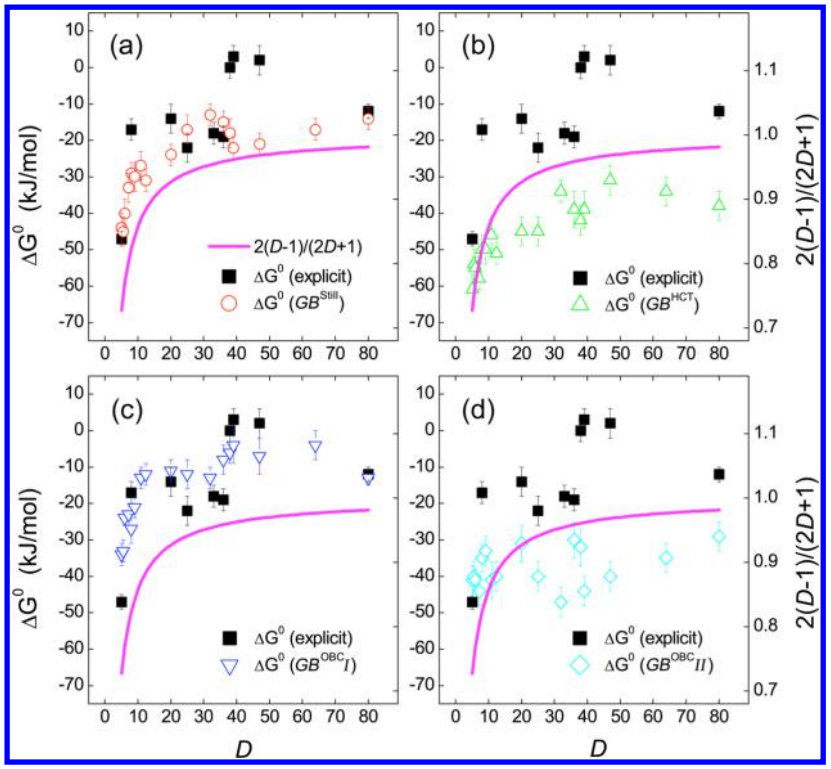

Figure 4. Binding free energy of β-CD dimerization (ΔG^0) versus dielectric constants (D) of the tested solvents with (a) GB^{Still}, (b) GB^{HCT}, (c) $GB^{OBC}I$, and (d) $GB^{OBC}II$ models. Results with explicit solvents are displayed in each panel for comparison. The solid line shows a function of $2(D-1)/(2D+1)$, indicative of its relationship with ΔG^0.

GB^{Still}, while producing a less negative PMF (i.e., a weaker binding of dimer) than GB^{Still}. In most cases the binding strength of β-CD dimer for the implicit models is on the order of GB^{HCT} > $GB^{OBC}II$ > GB^{Still} > $GB^{OBC}I$; the overestimation resulting from the former two models displays a relatively larger derivation from explicit simulations, revealing a limited applicability of GB^{HCT} and $GB^{OBC}II$ for the study of CD-containing systems.

Correlation of ΔG^0 with D. In order to evaluate the predictive power of D, binding free energies (ΔG^0) of β-CD dimerization with both explicit and implicit simulations were computed using eq 3 and plotted as a function of D in Figure 4. Since the change of electrostatic energy (A) in transferring a dipole molecule from a vacuum (D = 1) to a medium of dielectric constant D can be calculated by eq 5[55]

$$A = \frac{\mu^2}{3a^3}\cdot\frac{D-1}{2D+1} = A_{max}\cdot\frac{2(D-1)}{2D+1} \quad (5)$$

where $A_{max} = \mu^2/6a^3$, μ is the dipole moment, and a is the sphere radius. For illustrating the correlation of ΔG^0 with D, the function $y = 2(D-1)/(2D+1)$ is given by a solid magenta line in Figure 4. The binding strengths of the dimer in explicit and implicit solvation models differ significantly (Figure 4), although GB^{Still} and $GB^{OBC}I$ are reasonably close to explicit solvent simulations. The ΔG^0 for all the tested models are in the same order of magnitude, but the large overestimation for GB^{HCT} and $GB^{OBC}II$ indicates that these models need to be considered with caution. Figure 4 indicates that the correlation of ΔG^0 with D is not linear for GB^{Still}, GB^{HCT}, $GB^{OBC}I$, and $GB^{OBC}II$ models and that a large change in ΔG^0 is observed with D less than 20, which explains why we need more sample points for D in the range of [5, 20] (Table 1). A good relationship between ΔG^0 and $2(D-1)/(2D+1)$ is detected for GB^{Still} (Figure 4a), GB^{HCT} (Figure 4b), and $GB^{OBC}I$ (Figure 4c) models, while for $GB^{OBC}II$ (Figure 4d) ΔG^0 does not show any correlation with D.

To quantify such correlations further, ΔG^0 as a function of $2(D-1)/(2D+1)$ is presented in Figure 5 with a linear fit

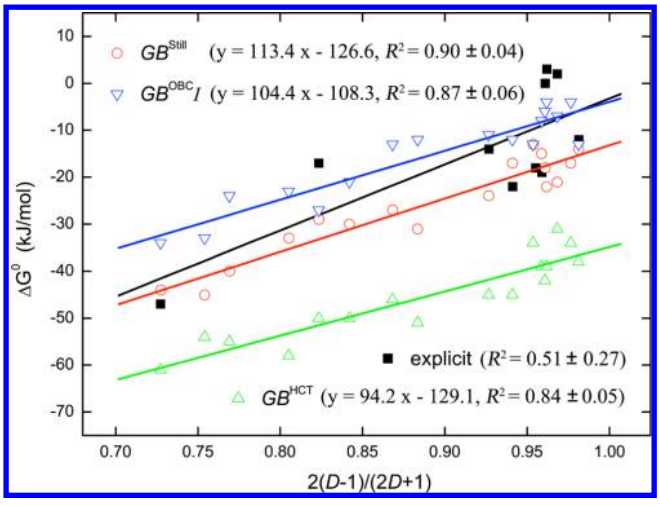

Figure 5. Binding free energy of β-CD dimerization (ΔG^0) as a function of $2(D-1)/(2D+1)$ where D is dielectric constant. For each solvation model, a linear fit to data points is plotted and R^2 is the correlation coefficient. The standard deviations in the correlation coefficients are determined by a bootstrapping analysis with 5000 iterations. Data for $GB^{OBC}II$ (R^2 = 0.14 ± 0.13) are not given here; errors of ΔG^0 (~4 kJ/mol) are considered for the fit but not presented for clarity.

DOI: 10.1021/acs.jctc.5b00620
J. Chem. Theory Comput. 2015, 11, 5103−5113

indicated by a solid line. For explicit simulations, the dimer binding (ΔG^0) only shows a weak correlation to dielectric constant (R^2 = 0.51 ± 0.27). The binding strength of β-CD dimer evaluated from GB^{Still}, GB^{HCT}, and $GB^{OBC}I$ models correlates much stronger with the dielectric constant ($R^2 \sim$ 0.9). The slope of the linear fits in Figure 5 may correspond to an effective A_{max} in eq 5, and the intercept may be relevant to van der Waals interactions (ΔG_{vdw}) and the energy of cavity formation (ΔG_{cav}) that are not included in eq 5. Although both these are solute properties, they do depend on the implicit solvent treatment. From Figures 4 and 5, we can see that all the *GB* models tested overestimate the dimer binding in high polar solvents such as DMSO, DMA, and DMF, which may be ascribed to the fact that implicit *GB* models fail to take account of the strong HB-interruption ability for such solvents.

Decomposition of Binding Energy. For a better understanding of the energy landscape driving β-CD dimerization, the binding energy of the two monomers along ξ (ΔE) was further decomposed (eq 4) and displayed in Figure 6 for chloroform and water simulations with GB^{Still}.

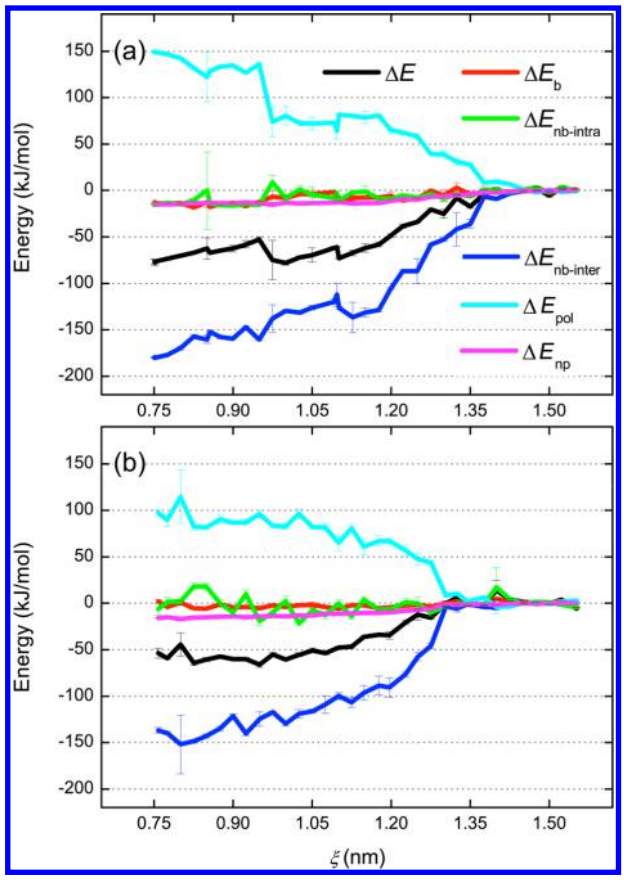

Figure 6. Landscape of binding energy (ΔE) and its decomposition during the process of β-CD dimerization for (a) chloroform and (b) water simulations with GB^{Still}. ΔE_b represents bonded interactions; $\Delta E_{nb\text{-}intra}$ for nonbonded intramolecular interactions; $\Delta E_{nb\text{-}inter}$ for nonbonded intermolecular interactions; ΔE_{pol} for polar contributions to ΔE; and ΔE_{np} for nonpolar contributions.

Association of two β-CD monomers may cause conformational changes to some extent, which is reflected in both the bonded (ΔE_b) and nonbonded intramolecular ($\Delta E_{nb\text{-}intra}$) interactions of the binding partners. Here ΔE_b only contains angle and dihedral terms because bond lengths of β-CD were kept rigid. $\Delta E_{nb\text{-}inter}$ denotes nonbonded intermolecular interactions (i.e., the sum of electrostatic and van der Waals between two β-CD monomers). ΔE_{pol} is CD-solvent electrostatic interactions, and ΔE_{np} is the sum of solvent−solvent cavity (ΔE_{cav}) and CD-solvent van der Waals (ΔE_{vdw}). ΔE_{pol} and ΔE_{vdw} together measure the desolvation of β-CD monomers upon association. As seen from Figure 6, conformational changes due to the association contribute little to the dimer binding, revealed by ΔE_b and $\Delta E_{nb\text{-}intra}$. The binding is largely due to $\Delta E_{nb\text{-}inter}$ and ΔE_{pol}, and ΔE_{np} tends to favor the binding. As expected, nonbonded interactions between β-CD monomers ($\Delta E_{nb\text{-}inter}$) favor the dimerization process, and $\Delta E_{nb\text{-}inter}$ in chloroform (Figure 6a) is more negative than in water (Figure 6b). A positive ΔE_{pol} implies that the two monomers are desolvated to a great extent during the association.

For a quantitative determination, binding energy (ΔE) and its components during the dimerization process are weighted by their Boltzmann factors (using eq 9 in ref 56). These weighed values as a function of D for all the *GB* models tested are displayed in Figure 7, allowing a direct comparison between these *GB* models. Data for explicit solvents comparable with implicit ones are given as well and indicated by a solid black line. For each *GB* model, a solid line obtained from 5-point-window adjacent averaging shows how ΔE varies with D for clarity.

As shown in Figure 7a, the total binding energy (ΔE) tends to be more negative (i.e., stronger binding) when D decreases and to be highly sensitive for D less than 10. For all the *GB* models tested, ΔE (Figure 7a) shows an order for the binding strength that is similar to ΔG^0 (Figure 4), and ΔE_b lies between −20 and 0 kJ/mol, favoring the dimerization (Figure 7b). $\Delta E_{nb\text{-}intra}$ for $GB^{OBC}I$ and $GB^{OBC}II$ tends to be positive disfavoring the monomer association, while for GB^{Still} and GB^{HCT} negative $\Delta E_{nb\text{-}intra}$ favors the binding (Figure 7c). It is generally assumed that binding partners adjust their configuration leading to a negative (favorable) $\Delta E_{nb\text{-}intra}$ for an effective complexation, as revealed by the explicit solvent simulations (Figure 7c). The GB^{OBC} model seems to contradict this assumption, and the resulting unfavorable $\Delta E_{nb\text{-}intra}$ is compensated somehow by a stronger interaction between the monomers (Figure 7d) and by a weaker electrostatic interaction between β-CD and solvent (Figure 7e). Given the scale of ΔE_{np}, there is no significant difference in nonpolar contributions for the tested GB models (Figure 7f).

Considering the five components of ΔE, overestimation for GB^{HCT} seems to be caused by stronger contributions from ΔE_b, $\Delta E_{nb\text{-}intra}$, and $\Delta E_{nb\text{-}inter}$; for $GB^{OBC}II$ mainly by a stronger $\Delta E_{nb\text{-}inter}$, although this strong interaction between two monomers is balanced by weaker ΔE_b and $\Delta E_{nb\text{-}intra}$. Compared to explicit simulations, the total binding energy (ΔE) with the GB models gives to a great extent an underestimation (Figure 7a). Implicit solvent models of GB^{Still} and $GB^{OBC}I$ appear to underestimate the interaction between two monomers ($\Delta E_{nb\text{-}inter}$) for solvents with low D and to overestimate it for polar solvents; however, estimation of this interaction with $GB^{OBC}II$ matches well with explicit simulations for the solvents with low polarity (Figure 7d). The *GB* models tested overestimate the electrostatic contribution from CD-solvent interactions (ΔE_{pol}, a major part of desolvation) for $CHCl_3$ (D = 5) in Figure 7e. For instance, explicit calculations in $CHCl_3$ give a much smaller ΔE_{pol} (~36 kJ/mol), while GB^{Still} gives a value of ~146 kJ/mol (Figure 6a). For the other solvents,

DOI: 10.1021/acs.jctc.5b00620
J. Chem. Theory Comput. 2015, 11, 5103−5113

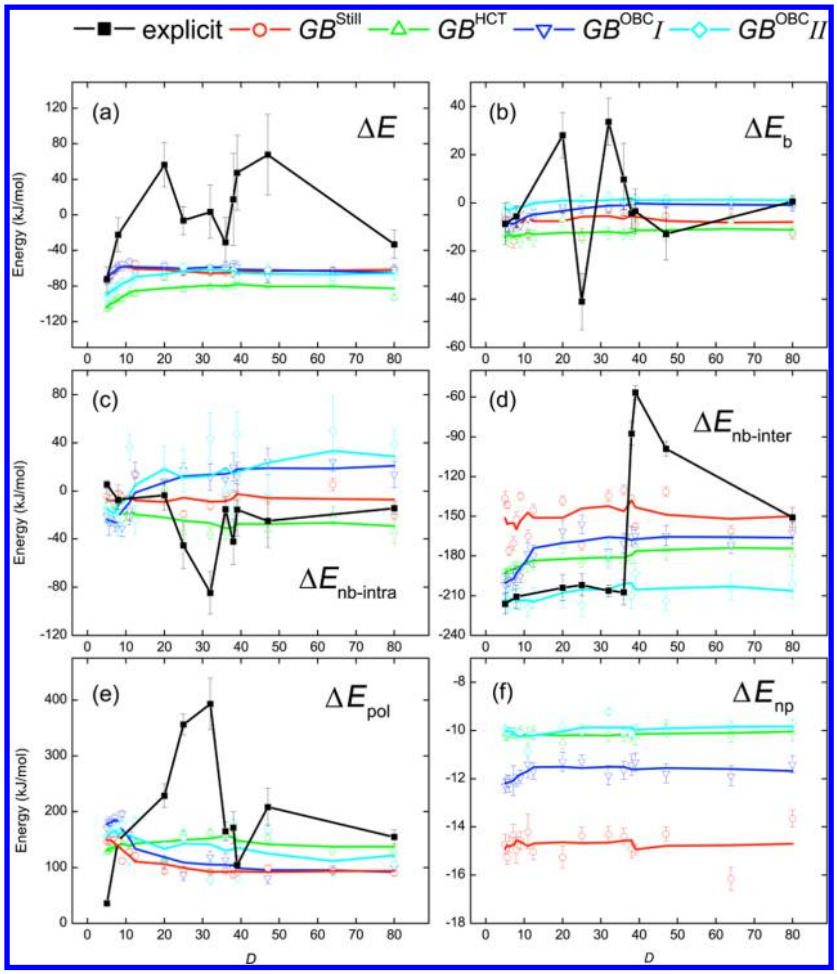

Figure 7. Binding energy (ΔE) and its components versus dielectric constants (D) for the tested *GB* solvation models. Data of explicit solvents comparable with implicit ones are given as well. Data points for *GB* models are smoothed by 5-point-window adjacent averaging and shown by solid lines.

however, the *GB* models seem to yield an underestimation (Figure 7e). In water, the explicit model produces a ΔE_{pol} of ~155 kJ/mol, but GB^{Still} is ~89 kJ/mol. ΔE_{pol} in the GB models totally decreases with the increasing D, which appears to go against the fact that hydroxyl groups of CDs prefer to interact with polar solvents (like HOH) rather than nonpolar ones (like $CHCl_3$), thus leading to a stronger desolvation upon association of two monomers in the polar solvents. The remaining two components of the total binding energy (ΔE) in explicit solvent calculations are the CD-solvent van der Waals interactions that disfavor binding and solvent−solvent interactions that favor the binding. Both are shown to contribute significantly to ΔE (Figure S5). These two contributions in implicit solvent models are proportional to the total solvent-accessible surface area (Table 2) and therefore have no corresponding terms in explicit solvent simulations.

DISCUSSION

Implicit solvent methods like generalized Born (GB) models have been designed and parametrized mainly for modeling an aqueous environment with a dielectric constant of ~80. The most important difference between various GB models is the way the effective Born radii are evaluated; in these models the Born radii depend only on the geometry of solute molecules but not on the dielectric environments of solute internally and of the external solvents.[3] Here our simulations in different dielectric constants (D) ranging from 5 to 80 neglect the external-environmental dependence of Born radii, introducing the risk of incorrect radii resulting from variable dielectric media. That is exactly the motivation of this work where we intend to address how well GB models approximate solvation in explicit organic solvents.

The tested models of GB^{Still}, GB^{HCT}, and GB^{OBC} correctly predict that the binding free energy (ΔG^0) of two β-CD monomers increases with the decreasing D (Figures 4 and 5), which agrees with the explicit solvent observation that the β-CD dimer showed a higher stability in lower polar solvents.[32] In addition, ΔG^0 with the GB models were on the same order of magnitude as that with explicit solvent models; a proper choice of GB models such as GB^{Still} and $GB^{OBC}I$ gives a reasonable estimate of ΔG^0 (Figures 4 and 5), although the details of the binding including hydrogen bonding are not well reproduced (Figure 2). These observations indicate that neglecting the environmental dependence of Born radii appears acceptable for such cyclodextrin calculations. When handling complex dielectric environments like lipid-membrane systems,[31] however, modifications of the atomic Born radii are required for accurate treatments of nonaqueous media in GB formalisms.[57−59]

The free energy of dimerization (ΔG^0) correlates strongly ($R^2 \sim 0.90$) with $2(D-1)/(2D+1)$, suggesting that D is a powerful predictor of ΔG^0 (Figure 5); however, this merely

DOI: 10.1021/acs.jctc.5b00620
J. Chem. Theory Comput. 2015, 11, 5103−5113

reflects the treatment of electrostatics in the Born equation, and hence this result is expected. For explicit solvent results only a weak correlation is observed ($R^2 \sim 0.50$), and almost no correlation is detected in high-dielectric solvents ($D > 20$), demonstrating that the Born equation does not hold for microscopic cases with structured solvents. In practice, the difference between the solvent models may lie in whether HB interruptions discussed above are modeled appropriately. In the range of $D < 10$ (Figure 4), ΔG^0 is very sensitive to D, which means in general that a slight variation in dielectric environment may lead to a large change in the solvation free energy for GB-based calculations, as demonstrated as well by Jacobson and co-workers.[60] They reported that a larger internal (solute) dielectric constant ($D = 2$) leads to a more significant and more positive enrichment than that with $D = 1$ (most of GB model parameters were optimized using this dielectric constant) during high-throughput docking for enriching known inhibitors to the estrogen receptor.[60] Biological membranes are believed to have different dielectric properties from protein ($D = 1-20$)[61−63] or water ($D = 80$). For implicit membrane modeling, for instance, DPPC bilayers were treated by four-dielectric layered regions with $D = 2$, 7, 180, and 210, respectively.[58] In this work, the high sensitivity of ΔG^0 to D in Figure 4 clearly indicates that low-dielectric environments (such as protein binding sites and membrane interiors) in implicit GB models are difficult to treat accurately.

The finding that GB^{HCT} gives a large overestimation of ΔG^0 (Figure 5) is not surprising since shortcomings have been reported for this method applied to macromolecules.[38] GB^{HCT} might underestimate the effective radii for buried atoms, resulting in too negative solvation energies for the compact regions in the solute.[38] GB^{OBC} has been developed to correct such shortcomings, and our results confirm that the ΔG^0 using this method is closer to the explicit solvent values (Figures 4 and 5). These findings also reveal that there are buried atoms in the binding interface of two β-CD monomers, which involve the complementary networks of hydrogen bonds.[32] Somewhat unexpectedly, $GB^{OBC}II$ behaves differently from $GB^{OBC}I$ and overestimates the binding free energy (Figure 4d). Large discrepancies in ΔG^0 between explicit solvent and implicit GB models occur mostly in high-polar solvents such as DMSO, DMA, and DMF (Figure 2). These solvents act as strong hydrogen bond (HB) acceptors and hence have the ability to interrupt HB interactions between two β-CD monomers.[32] Such HB interruptions are difficult to model using continuum methods such as PB or GB. The reason for this is that the properties of real solvent molecules, like discrete hydrogen bonding sites (e.g., that a solvent can make just one hydrogen bond) and directionality of dipoles, are difficult to describe analytically.[64] There are many reports pointing out problems with implicit solvent models in protein simulations, such as charged residues,[5,27] water-induced core collapse and desolvation,[19] water-mediated HBs,[65] and calculations of ligand binding free energies.[66,67] Some improvement to ligand binding energy calculations can be made by introducing a number of explicit water molecules as part of the binding site;[68] however, it is not trivial to determine where those water molecules need to be placed.[69] More detailed information would need to be incorporated into implicit solvent models, in particular, for the HB forming ability of solvents to overcome these problems; it is not clear how this could be done, however.

The decomposition of binding energy presented in Figures 6 and 7 quantifies the individual contributions from the solute itself and implicit solvents to the total binding (ΔE) and showcases the differences between explicit and implicit solvent representations in detail. Unfavorable desolvation (ΔE_{pol}) of the solute and favorable intermolecular interactions ($\Delta E_{nb\text{-}inter}$) upon association are observed both in implicit and explicit solvent simulations. However, it is quite surprising that the polar contributions (ΔE_{pol}) to ΔE in low-dielectric media are larger than in high-dielectric solvents for the GB models (Figure 7e), in contrast to the observation in explicit solvents that ΔE_{pol} is larger at higher D (Figure 7). In addition, the contributions of nonbonded intramolecular interactions ($\Delta E_{nb\text{-}intra}$) due to change in configuration upon complexation appear to depend on the GB models. $\Delta E_{nb\text{-}intra}$ in GB^{Still} and GB^{HCT} favor dimerization of β-CD monomers, while $\Delta E_{nb\text{-}intra}$ in GB^{OBC} does the opposite. These differences may be ascribed to the fact that solvent−solvent interactions are described implicitly in the components of ΔE in a different manner.

In this work we have compared the ability of implicit solvent models to reproduce the potential of mean force for β-CD dimerization obtained in explicit solvent models. The results showed that generalized Born (GB) implicit models may fail in media where hydrogen bonds are of importance and that GB-based evaluations are very sensitive to the dielectric constant in low-dielectric environments. ΔG^0 of β-CD dimerization with GB models correlates strongly ($R^2 \sim 0.90$) with $2(D-1)/(2D+1)$, while explicit solvent simulations give a very weak correlation only ($R^2 \sim 0.50$). In order to study this more in-depth, we examined solvation free energies (ΔG_{sol}) of small organic molecules (such as acetone, methanol, ethanol, and chloroform) in different organic media and found that ΔG_{sol}, for both experimental observations and explicit solvent simulations, have very weak correlations ($R^2 = 0.07-0.63$) with $2(D-1)/(2D+1)$ as well (Table 3). These findings indicate that such correlations are system-dependent rather than general for realistic systems.

Table 3. Correlation of Solvation Free Energy (ΔG_{sol}) of Solutes in Different Organic Solvents with $2(D-1)/(2D+1)$[a]

solute	no. of solvents	correlation (R^2)[b] exp.	correlation (R^2)[b] explicit sims.
acetone	17	0.30 ± 0.18	0.29 ± 0.20
acetonitrile	12	0.07 ± 0.13	0.08 ± 0.15
chloroform	15	0.06 ± 0.08	0.19 ± 0.16
dichloromethane	14	0.11 ± 0.12	0.13 ± 0.16
ethanol	19	0.50 ± 0.16	0.44 ± 0.19
methanol	17	0.63 ± 0.18	0.50 ± 0.18
nitromethane	12	0.11 ± 0.15	0.12 ± 0.18
toluene	17	0.24 ± 0.17	0.28 ± 0.23

[a] ΔG_{sol} were taken from ref 29 and references therein. [b] Standard deviations in R^2 were determined by a bootstrapping analysis with 5000 iterations.

The GB radii used depend on the details of the complex (which could change with dielectric media), and the free energy of binding also entails other terms than electrostatic contributions, such as the size and dipole of the solute and the surface tension of the solvent that would be different from case to case.[70] However, as follows from eq 5, the first two of these are solute properties which can therefore not explain the low correlation between ΔG^0 and $2(D-1)/(2D+1)$ in real systems. The surface tension of the solvent, which is important for the free energy of cavity formation, is a nonlinear function

DOI: 10.1021/acs.jctc.5b00620
J. Chem. Theory Comput. 2015, 11, 5103−5113

of the size of the cavity,[71] further complicating analytical analysis. It is hard to see that this parameter alone could be responsible for the low correlation between the Onsager relation and Gibbs energies of solvation.

In addition, GB models fit parameters to reproduce results obtained by Poisson−Boltzmann (PB) models, typically assuming the molecular surface as the boundary for assignment of the internal and external dielectric constants.[72] A probe radius of solvent (0.14 nm for water, for instance) is generally used to augment the van der Waals (vdW) surface for construction of molecular surface (such as Lee-Richards model).[73] If the probe radii (solvent size) are similar, the results should not depend on it very much. All the nonaqueous solvent molecules tested in this work are larger than water and therefore have less contact with the solutes, as shown by the Molinspiration calculation of molecular volumes (Table S1). GB-based calculations that do not take into account the solvent size could result in a loss in accuracy compared to PB models, although PB is not always a gold standard. The development of implicit solvent models has, particularly in quantum chemistry,[74,75] improved recently based on an earlier work by York and Karplus.[76] In these models more parameters (such as solvent radius and density) than just the dielectric constants are used to model solvents other than water. Nevertheless it seems that the Onsager reaction field,[70] which is the foundation for most implicit solvent models, does not hold for real solvents and solutes (Table 3).

It should be kept in mind that most simplified models, including implicit solvent models and coarse-grained models, are not tuned to reproduce explicit solvent results but rather experimental data. This is reasonable since explicit solvents are not perfect either. In that respect it would be useful to benchmark the performance of implicit solvent models to explicit solvents where there is experimental data available as well, as was done recently by computing solvation energies using thermodynamic integration and comparing the results to quantitative structure property relations and to the conductor-like screening models for realistic solvation.[29] An analysis of the performance of implicit solvents for the computation of solvation energies in different solvents would give further insight into the predictive power of these models in nonaqueous environments.

■ ASSOCIATED CONTENT

Supporting Information

The Supporting Information is available free of charge on the ACS Publications website at DOI: 10.1021/acs.jctc.5b00620.

Figures S1−S6, Tables S1 and S2 (PDF)

■ AUTHOR INFORMATION

Corresponding Author

*Phone: 46 18 471 4205. E-mail: david.vanderspoel@icm.uu.se.

Notes

The authors declare no competing financial interest.

■ ACKNOWLEDGMENTS

A grant of computer time by ChemCloudComputing of BUCT is acknowledged. This work was supported by the Fundamental Research Funds for the Central Universities (FRF-TP-15-018A1), the National Basic Research Program of China (973 program: 2013CB733600 and 2012CB72520) and the National Nature Science Foundation of China (21390202, 21436002, and 21306006) as well as by the Swedish Research Council (grant 2013-5947).

■ REFERENCES

(1) Roux, B.; Simonson, T. Implicit Solvent Models. *Biophys. Chem.* **1999**, *78*, 1−20.

(2) Feig, M.; Brooks, C. L., III Recent Advances in the Development and Application of Implicit Solvent Models in Biomolecule Simulations. *Curr. Opin. Struct. Biol.* **2004**, *14*, 217−224.

(3) Chen, J.; Brooks, C. L., III; Khandogin, J. Recent Advances in Implicit Solvent-Based Methods for Biomolecular Simulations. *Curr. Opin. Struct. Biol.* **2008**, *18*, 140−148.

(4) Kleinjung, J.; Fraternali, F. Design and Application of Implicit Solvent Models in Biomolecular Simulations. *Curr. Opin. Struct. Biol.* **2014**, *25*, 126−134.

(5) Zhou, R.; Berne, B. J. Can a Continuum Solvent Model Reproduce the Free Energy Landscape of a β-Hairpin Folding in Water? *Proc. Natl. Acad. Sci. U. S. A.* **2002**, *99*, 12777−12782.

(6) Snow, C. D.; Nguyen, H.; Pande, V. S.; Gruebele, M. Absolute Comparison of Simulated and Experimental Protein-Folding Dynamics. *Nature* **2002**, *420*, 102−106.

(7) Nguyen, H.; Maier, J.; Huang, H.; Perrone, V.; Simmerling, C. Folding Simulations for Proteins with Diverse Topologies Are Accessible in Days with a Physics-Based Force Field and Implicit Solvent. *J. Am. Chem. Soc.* **2014**, *136*, 13959−13962.

(8) Schwarzl, S. M.; Tschopp, T. B.; Smith, J. C.; Fischer, S. Can the Calculation of Ligand Binding Free Energies Be Improved with Continuum Solvent Electrostatics and an Ideal-Gas Entropy Correction? *J. Comput. Chem.* **2002**, *23*, 1143−1149.

(9) Michel, J.; Verdonk, M. L.; Essex, J. W. Protein-Ligand Binding Affinity Predictions by Implicit Solvent Simulations: A Tool for Lead Optimization? *J. Med. Chem.* **2006**, *49*, 7427−7439.

(10) Guo, Z.; Li, B.; Cheng, L.-T.; Zhou, S.; McCammon, J. A.; Che, J. Identification of Protein−Ligand Binding Sites by the Level-Set Variational Implicit-Solvent Approach. *J. Chem. Theory Comput.* **2015**, *11*, 753−765.

(11) Cortis, C. M.; Friesner, R. A. Numerical Solution of the Poisson-Boltzmann Equation Using Tetrahedral Finite-Element Meshes. *J. Comput. Chem.* **1997**, *18*, 1591−1608.

(12) Koehl, P. Electrostatics Calculations: Latest Methodological Advances. *Curr. Opin. Struct. Biol.* **2006**, *16*, 142−151.

(13) Hawkins, G. D.; Cramer, C. J.; Truhlar, D. G. Pairwise Solute Descreening of Solute Charges from a Dielectric Medium. *Chem. Phys. Lett.* **1995**, *246*, 122−129.

(14) Tsui, V.; Case, D. A. Theory and Applications of the Generalized Born Solvation Model in Macromolecular Simulations. *Biopolymers* **2000**, *56*, 275−291.

(15) Knight, J. L.; Brooks, C. L. Surveying Implicit Solvent Models for Estimating Small Molecule Absolute Hydration Free Energies. *J. Comput. Chem.* **2011**, *32*, 2909−2923.

(16) Feig, M.; Onufriev, A.; Lee, M. S.; Im, W.; Case, D. A.; Brooks, C. L. Performance Comparison of Generalized Born and Poisson Methods in the Calculation of Electrostatic Solvation Energies for Protein Structures. *J. Comput. Chem.* **2004**, *25*, 265−284.

(17) Liu, H.-Y.; Zou, X. Electrostatics of Ligand Binding: Parametrization of the Generalized Born Model and Comparison with the Poisson−Boltzmann Approach. *J. Phys. Chem. B* **2006**, *110*, 9304−9313.

(18) Nguyen, H.; Roe, D. R.; Simmerling, C. Improved Generalized Born Solvent Model Parameters for Protein Simulations. *J. Chem. Theory Comput.* **2013**, *9*, 2020−2034.

(19) Rhee, Y. M.; Sorin, E. J.; Jayachandran, G.; Lindahl, E.; Pande, V. S. Simulations of the Role of Water in the Protein-Folding Mechanism. *Proc. Natl. Acad. Sci. U. S. A.* **2004**, *101*, 6456−6461.

(20) Nymeyer, H.; García, A. E. Simulation of the Folding Equilibrium of α-Helical Peptides: A Comparison of the Generalized Born Approximation with Explicit Solvent. *Proc. Natl. Acad. Sci. U. S. A.* **2003**, *100*, 13934−13939.

DOI: 10.1021/acs.jctc.5b00620
J. Chem. Theory Comput. 2015, 11, 5103−5113

(21) Zhou, R. Free Energy Landscape of Protein Folding in Water: Explicit vs. Implicit Solvent. *Proteins: Struct., Funct., Genet.* **2003**, *53*, 148−161.
(22) Huang, N.; Kalyanaraman, C.; Irwin, J. J.; Jacobson, M. P. Physics-Based Scoring of Protein−Ligand Complexes: Enrichment of Known Inhibitors in Large-Scale Virtual Screening. *J. Chem. Inf. Model.* **2006**, *46*, 243−253.
(23) Greenidge, P. A.; Kramer, C.; Mozziconacci, J. C.; Sherman, W. Improving Docking Results Via Reranking of Ensembles of Ligand Poses in Multiple X-Ray Protein Conformations with MM-GBSA. *J. Chem. Inf. Model.* **2014**, *54*, 2697−2717.
(24) Zhang, X.; Wong, S. E.; Lightstone, F. C. Toward Fully Automated High Performance Computing Drug Discovery: A Massively Parallel Virtual Screening Pipeline for Docking and Molecular Mechanics/Generalized Born Surface Area Rescoring to Improve Enrichment. *J. Chem. Inf. Model.* **2014**, *54*, 324−337.
(25) Onufriev, A. Implicit Solvent Models in Molecular Dynamics Simulations: A Brief Overview. In *Annual Reports in Computational Chemistry*; Ralph, A. W.; David, C. S., Eds.; Elsevier: 2008; Vol. *4*, pp 125−137.
(26) Fan, H.; Mark, A. E.; Zhu, J.; Honig, B. Comparative Study of Generalized Born Models: Protein Dynamics. *Proc. Natl. Acad. Sci. U. S. A.* **2005**, *102*, 6760−6764.
(27) Zeller, F.; Zacharias, M. Evaluation of Generalized Born Model Accuracy for Absolute Binding Free Energy Calculations. *J. Phys. Chem. B* **2014**, *118*, 7467−7474.
(28) Duffy, E. M.; Jorgensen, W. L. Prediction of Properties from Simulations: Free Energies of Solvation in Hexadecane, Octanol, and Water. *J. Am. Chem. Soc.* **2000**, *122*, 2878−2888.
(29) Zhang, J.; Tuguldur, B.; van der Spoel, D. Force Field Benchmark of Organic Liquids. 2. Gibbs Energy of Solvation. *J. Chem. Inf. Model.* **2015**, *55*, 1192−1201.
(30) Gaillard, T.; Case, D. A. Evaluation of DNA Force Fields in Implicit Solvation. *J. Chem. Theory Comput.* **2011**, *7*, 3181−3198.
(31) Grossfield, A. Implicit Modeling of Membranes. In *Current Topics in Membranes*; Scott, E. F., Ed.; Academic Press: 2008; Vol. *60*, pp 131−157.
(32) Zhang, H.; Tan, T.; Feng, W.; van der Spoel, D. Molecular Recognition in Different Environments: β-Cyclodextrin Dimer Formation in Organic Solvents. *J. Phys. Chem. B* **2012**, *116*, 12684−12693.
(33) van de Manakker, F.; Vermonden, T.; van Nostrum, C. F.; Hennink, W. E. Cyclodextrin-Based Polymeric Materials: Synthesis, Properties, and Pharmaceutical/Biomedical Applications. *Biomacromolecules* **2009**, *10*, 3157−3175.
(34) Fan, Z.; Diao, C.-H.; Song, H.-B.; Jing, Z.-L.; Yu, M.; Chen, X.; Guo, M.-J. Encapsulation of Quinine by β-Cyclodextrin: Excellent Model for Mimicking Enzyme−Substrate Interactions. *J. Org. Chem.* **2006**, *71*, 1244−1246.
(35) Knowles, T. P.; Fitzpatrick, A. W.; Meehan, S.; Mott, H. R.; Vendruscolo, M.; Dobson, C. M.; Welland, M. E. Role of Intermolecular Forces in Defining Material Properties of Protein Nanofibrils. *Science* **2007**, *318*, 1900−1903.
(36) Qiu, D.; Shenkin, P. S.; Hollinger, F. P.; Still, W. C. The GB/SA Continuum Model for Solvation. A Fast Analytical Method for the Calculation of Approximate Born Radii. *J. Phys. Chem. A* **1997**, *101*, 3005−3014.
(37) Hawkins, G. D.; Cramer, C. J.; Truhlar, D. G. Parametrized Models of Aqueous Free Energies of Solvation Based on Pairwise Descreening of Solute Atomic Charges from a Dielectric Medium. *J. Phys. Chem.* **1996**, *100*, 19824−19839.
(38) Onufriev, A.; Bashford, D.; Case, D. A. Exploring Protein Native States and Large-Scale Conformational Changes with a Modified Generalized Born Model. *Proteins: Struct., Funct., Genet.* **2004**, *55*, 383−394.
(39) Wang, E.; Chen, G.; Han, C. Crystal Structures of β-Cyclodextrin Inclusion Complexes with 7-Hydroxycoumarin and 4-Hydroxycoumarin and Substituent Effects on Inclusion Geometry. *Chin. J. Chem.* **2011**, *29*, 617−622.
(40) Hess, B.; Kutzner, C.; van der Spoel, D.; Lindahl, E. GROMACS 4: Algorithms for Highly Efficient, Load-Balanced, and Scalable Molecular Simulation. *J. Chem. Theory Comput.* **2008**, *4*, 435−447.
(41) van der Spoel, D.; Lindahl, E.; Hess, B.; Groenhof, G.; Mark, A. E.; Berendsen, H. J. C. GROMACS: Fast, Flexible, and Free. *J. Comput. Chem.* **2005**, *26*, 1701−1718.
(42) Pronk, S.; Páll, S.; Schulz, R.; Larsson, P.; Bjelkmar, P.; Apostolov, R.; Shirts, M. R.; Smith, J. C.; Kasson, P. M.; van der Spoel, D.; Hess, B.; Lindahl, E. GROMACS 4.5: A High-Throughput and Highly Parallel Open Source Molecular Simulation Toolkit. *Bioinformatics* **2013**, *29*, 845−854.
(43) Bussi, G.; Donadio, D.; Parrinello, M. Canonical Sampling through Velocity Rescaling. *J. Chem. Phys.* **2007**, *126*, 014101.
(44) Hess, B.; Bekker, H.; Berendsen, H. J. C.; Fraaije, J. G. E. M. Lincs: A Linear Constraint Solver for Molecular Simulations. *J. Comput. Chem.* **1997**, *18*, 1463−1472.
(45) Cezard, C.; Trivelli, X.; Aubry, F.; Djedaini-Pilard, F.; Dupradeau, F. Y. Molecular Dynamics Studies of Native and Substituted Cyclodextrins in Different Media: 1. Charge Derivation and Force Field Performances. *Phys. Chem. Chem. Phys.* **2011**, *13*, 15103−15121.
(46) Larsson, P.; Lindahl, E. A High-Performance Parallel-Generalized Born Implementation Enabled by Tabulated Interaction Rescaling. *J. Comput. Chem.* **2010**, *31*, 2593−2600.
(47) Schaefer, M.; Bartels, C.; Karplus, M. Solution Conformations and Thermodynamics of Structured Peptides: Molecular Dynamics Simulation with an Implicit Solvation Model. *J. Mol. Biol.* **1998**, *284*, 835−848.
(48) Kumar, S.; Rosenberg, J. M.; Bouzida, D.; Swendsen, R. H.; Kollman, P. A. The Weighted Histogram Analysis Method for Free-Energy Calculations on Biomolecules. I. The Method. *J. Comput. Chem.* **1992**, *13*, 1011−1021.
(49) Hub, J. S.; de Groot, B. L.; van der Spoel, D. g_wham−A Free Weighted Histogram Analysis Implementation Including Robust Error and Autocorrelation Estimates. *J. Chem. Theory Comput.* **2010**, *6*, 3713−3720.
(50) Auletta, T.; de Jong, M. R.; Mulder, A.; van Veggel, F. C. J. M.; Huskens, J.; Reinhoudt, D. N.; Zou, S.; Zapotoczny, S.; Schönherr, H.; Vancso, G. J.; Kuipers, L. β-Cyclodextrin Host−Guest Complexes Probed under Thermodynamic Equilibrium: Thermodynamics and Afm Force Spectroscopy. *J. Am. Chem. Soc.* **2004**, *126*, 1577−1584.
(51) Yu, Y.; Chipot, C.; Cai, W.; Shao, X. Molecular Dynamics Study of the Inclusion of Cholesterol into Cyclodextrins. *J. Phys. Chem. B* **2006**, *110*, 6372−6378.
(52) Darden, T.; York, D.; Pedersen, L. Particle Mesh Ewald: An *N*·log(*N*) Method for Ewald Sums in Large Systems. *J. Chem. Phys.* **1993**, *98*, 10089−10092.
(53) Essmann, U.; Perera, L.; Berkowitz, M. L.; Darden, T.; Lee, H.; Pedersen, L. G. A Smooth Particle Mesh Ewald Method. *J. Chem. Phys.* **1995**, *103*, 8577−8593.
(54) Hess, B. Determining the Shear Viscosity of Model Liquids from Molecular Dynamics Simulations. *J. Chem. Phys.* **2002**, *116*, 209−217.
(55) Bell, R. P. The Electrostatic Energy of Dipole Molecules in Different Media. *Trans. Faraday Soc.* **1931**, *27*, 797−802.
(56) Zhang, H.; Tan, T.; Hetényi, C.; van der Spoel, D. Quantification of Solvent Contribution to the Stability of Noncovalent Complexes. *J. Chem. Theory Comput.* **2013**, *9*, 4542−4551.
(57) Feig, M.; Im, W.; Brooks, C. L. Implicit Solvation Based on Generalized Born Theory in Different Dielectric Environments. *J. Chem. Phys.* **2004**, *120*, 903−911.
(58) Tanizaki, S.; Feig, M. A Generalized Born Formalism for Heterogeneous Dielectric Environments: Application to the Implicit Modeling of Biological Membranes. *J. Chem. Phys.* **2005**, *122*, 124706.
(59) Tanizaki, S.; Feig, M. Molecular Dynamics Simulations of Large Integral Membrane Proteins with an Implicit Membrane Model. *J. Phys. Chem. B* **2006**, *110*, 548−556.
(60) Huang, N.; Kalyanaraman, C.; Bernacki, K.; Jacobson, M. P. Molecular Mechanics Methods for Predicting Protein-Ligand Binding. *Phys. Chem. Chem. Phys.* **2006**, *8*, 5166−5177.

DOI: 10.1021/acs.jctc.5b00620
J. Chem. Theory Comput. 2015, 11, 5103−5113

(61) Schutz, C. N.; Warshel, A. What Are the Dielectric "Constants" of Proteins and How to Validate Electrostatic Models? *Proteins: Struct., Funct., Genet.* **2001**, *44*, 400−417.
(62) Boas, F. E.; Harbury, P. B. Potential Energy Functions for Protein Design. *Curr. Opin. Struct. Biol.* **2007**, *17*, 199−204.
(63) Dwyer, J. J.; Gittis, A. G.; Karp, D. A.; Lattman, E. E.; Spencer, D. S.; Stites, W. E.; García-Moreno, E. B. High Apparent Dielectric Constants in the Interior of a Protein Reflect Water Penetration. *Biophys. J.* **2000**, *79*, 1610−1620.
(64) Hub, J. S.; Wolf, M. G.; Caleman, C.; van Maaren, P. J.; Groenhof, G.; van der Spoel, D. Thermodynamics of Hydronium and Hydroxide Surface Solvation. *Chem. Sci.* **2014**, *5*, 1745−1749.
(65) García, A. E.; Sanbonmatsu, K. Y. Exploring the Energy Landscape of a β Hairpin in Explicit Solvent. *Proteins: Struct., Funct., Genet.* **2001**, *42*, 345−354.
(66) Godschalk, F.; Genheden, S.; Soderhjelm, P.; Ryde, U. Comparison of MM/GBSA Calculations Based on Explicit and Implicit Solvent Simulations. *Phys. Chem. Chem. Phys.* **2013**, *15*, 7731−7739.
(67) Genheden, S.; Ryde, U. The MM/PBSA and MM/GBSA Methods to Estimate Ligand-Binding Affinities. *Expert Opin. Drug Discovery* **2015**, *10*, 449−461.
(68) Mikulskis, P.; Genheden, S.; Ryde, U. Effect of Explicit Water Molecules on Ligand-Binding Affinities Calculated with the MM/GBSA Approach. *J. Mol. Model.* **2014**, *20*, 1−11.
(69) Jeszenői, N.; Horváth, I.; Bálint, M.; van der Spoel, D.; Hetényi, C. Mobility-Based Prediction of Hydration Structures of Protein Surfaces. *Bioinformatics* **2015**, *31*, 1959−1965.
(70) Onsager, L. Electric Moments of Molecules in Liquids. *J. Am. Chem. Soc.* **1936**, *58*, 1486−1493.
(71) Wu, J. Solvation of a Spherical Cavity in Simple Liquids: Interpolating between the Limits. *J. Phys. Chem. B* **2009**, *113*, 6813−6818.
(72) Rocchia, W.; Sridharan, S.; Nicholls, A.; Alexov, E.; Chiabrera, A.; Honig, B. Rapid Grid-Based Construction of the Molecular Surface and the Use of Induced Surface Charge to Calculate Reaction Field Energies: Applications to the Molecular Systems and Geometric Objects. *J. Comput. Chem.* **2002**, *23*, 128−137.
(73) Lee, B.; Richards, F. M. The Interpretation of Protein Structures: Estimation of Static Accessibility. *J. Mol. Biol.* **1971**, *55*, 379−400.
(74) Scalmani, G.; Frisch, M. J. Continuous Surface Charge Polarizable Continuum Models of Solvation. I. General Formalism. *J. Chem. Phys.* **2010**, *132*, 114110.
(75) Tomasi, J.; Mennucci, B.; Cammi, R. Quantum Mechanical Continuum Solvation Models. *Chem. Rev.* **2005**, *105*, 2999−3094.
(76) York, D. M.; Karplus, M. A Smooth Solvation Potential Based on the Conductor-Like Screening Model. *J. Phys. Chem. A* **1999**, *103*, 11060−11079.

DOI: 10.1021/acs.jctc.5b00620
J. Chem. Theory Comput. 2015, 11, 5103−5113